

# PROCEEDINGS OF SPIE

[SPIDigitalLibrary.org/conference-proceedings-of-spie](https://spiedigitallibrary.org/conference-proceedings-of-spie)

## Preliminary surface charging analysis of Ariel payload dielectrics in early transfer orbit and L2-relevant space environment

M. Focardi, M. Michelagnoli, V. Noce, M. Vela Nunez, P. Bolli, et al.

M. Focardi, M. Michelagnoli, V. Noce, M. Vela Nunez, P. Bolli, R. Nesti, A. Lorenzani, L. Carbonaro, C. Del Vecchio, G. Falcini, A. Tozzi, A. Di Giorgio, E. Galli, M. Farina, G. Giusi, S. J. Liu, M. Venter, E. Tommasi, F. De Persio, M. Salatti, D. Brienza, R. Piazzolla, G. Morgante, N. Auricchio, E. Pascale, L. Naponiello, G. Redigonda, E. Pace, G. Preti, G. Micela, G. Malaguti, P. Eccleston, A. Caldwell, G. Bishop, L. Desjonqueres, G. Tinetti, "Preliminary surface charging analysis of Ariel payload dielectrics in early transfer orbit and L2-relevant space environment," Proc. SPIE 12180, Space Telescopes and Instrumentation 2022: Optical, Infrared, and Millimeter Wave, 1218047 (27 August 2022); doi: 10.1117/12.2628170

**SPIE.**

Event: SPIE Astronomical Telescopes + Instrumentation, 2022, Montréal, Québec, Canada

# Preliminary surface charging analysis of the Ariel Payload dielectrics in early transfer orbit and L2-relevant space environment

M. Focardi<sup>\*a</sup>, M. Michelagnoli<sup>b</sup>, V. Noce<sup>a</sup>, M. Vela Nunez<sup>a</sup>, P. Bolli<sup>a</sup>, R. Nesti<sup>a</sup>, A. Lorenzani<sup>a</sup>, L. Carbonaro<sup>a</sup>, C. Del Vecchio<sup>a</sup>, G. Falcini<sup>a</sup>, A. Tozzi<sup>a</sup>, A. Di Giorgio<sup>c</sup>, E. Galli<sup>c</sup>, M. Farina<sup>c</sup>, G. Giusi<sup>c</sup>, S.J. Liu<sup>c</sup>, M. Venter<sup>l</sup>, E. Tommasi<sup>d</sup>, F. De Persio<sup>d</sup>, M. Salatti<sup>d</sup>, D. Brienza<sup>d</sup>, R. Piazzolla<sup>d</sup>, G. Morgante<sup>g</sup>, N. Auricchio<sup>g</sup>, E. Pascale<sup>e</sup>, L. Naponiello<sup>b</sup>, G. Redigonda<sup>b</sup>, E. Pace<sup>b</sup>, G. Preti<sup>b</sup>, G. Micela<sup>f</sup>, G. Malaguti<sup>g</sup>, P. Eccleston<sup>h</sup>, A. Caldwell<sup>h</sup>, G. Bishop<sup>h</sup>, L. Desjonquieres<sup>h</sup>, G. Tinetti<sup>i</sup>  
and the

Ariel Mission Consortium (AMC)

<sup>a</sup>INAF/OAA Arcetri Astrophysical Observatory, Largo E. Fermi 5, 50125 Firenze - IT

<sup>b</sup>University of Florence - Department of Physics and Astronomy, Largo E. Fermi 2, 50125 Firenze - IT

<sup>c</sup>INAF/IAPS Institute of Space Astrophysics and Planetology, Via del F. del Cavaliere 100, 00133 Roma - IT

<sup>d</sup>ASI - Italian Space Agency, Via del Politecnico, 00133 Roma - IT

<sup>e</sup>University of Rome - La Sapienza, Piazzale Aldo Moro 5, 00185 Roma - IT

<sup>f</sup>INAF/OAPa Astronomical Observatory of Palermo, Piazza del Parlamento 1, 90134 Palermo - IT

<sup>g</sup>INAF/OAS Astrophysics and Space Science Observatory, Via P. Gobetti 101, 40129 Bologna - IT

<sup>h</sup>STFC/RAL Space - Rutherford Appleton Laboratory, OX11 0QX Harwell Oxford - UK

<sup>i</sup>UCL - University College of London, Gower St, London WC1E 6BT - UK

<sup>l</sup>SARAO - South African Radio Astronomy Observatory, Black River Park North, Cape Town, 7925 - SA

## ABSTRACT

Ariel [1] is the M4 mission of the ESA's Cosmic Vision Program 2015-2025, whose aim is to characterize by low-resolution transit spectroscopy the atmospheres of over one thousand warm and hot exoplanets orbiting nearby stars.

The operational orbit of the spacecraft is baselined as a large amplitude halo orbit around the Sun-Earth L2 Lagrangian point, as it offers the possibility of long uninterrupted observations in a fairly stable radiative and thermo-mechanical environment. A direct escape injection with a single passage through the Earth radiation belts and no eclipses is foreseen.

The space environment around Earth and L2 presents significant design challenges to all spacecraft, including the effects of interactions with Sun radiation and charged particles owing to the surrounding plasma environment, potentially leading to dielectrics charging and unwanted electrostatic discharge (ESD) phenomena endangering the Payload operations and its data integrity.

Here, we present some preliminary simulations and analyses about the Ariel Payload dielectrics and semiconductors charging along the transfer orbit from launch to L2 included.

**Keywords:** Exoplanets, Transit Spectroscopy, Atmospheres, Payload, Dielectrics Charging, ESD – Electrostatic Discharge

## 1. INTRODUCTION

Ariel, the Atmospheric Remote-Sensing Infrared Exoplanet Large-survey satellite, is the ESA's Cosmic Vision M4 mission, selected in March 2018 and adopted by the Agency in November 2020 for a launch in early 2029, whose aim is

---

\*mauro.focardi@inaf.it; phone +39 055 2752 260

to characterize by low-resolution transit spectroscopy and spectrophotometry the atmospheres of over one thousand warm and hot exoplanets orbiting nearby stars.

The Ariel Payload (P/L) has been designed to perform transit spectroscopy from space during primary and secondary planetary eclipses in order to achieve a large unbiased survey concerning the nature of exoplanets atmospheres and their interiors and to determine the key factors affecting the formation and evolution of planetary systems.

Ariel will observe hundreds of warm and hot transiting gas giants, Neptunes and super-Earths around a wide range of host star types, targeting planets hotter than  $\sim 600$  K to take advantage of their well-mixed atmospheres. It will exploit primary and secondary transit spectroscopy in the  $1.10$  to  $7.80 \mu\text{m}$  spectral range and broadband photometry in the optical ( $0.50 - 0.80 \mu\text{m}$ ) and Near IR ( $0.80 - 1.10 \mu\text{m}$ ).

One of the two instruments of the Ariel Payload, contributing to the Spacecraft (S/C) Attitude and Orbit Control System (AOCS) operations, is the Fine Guidance System (FGS), including three photometric channels (two used for guiding as well as science) between  $0.5-1.1 \mu\text{m}$  plus a low resolution NIR spectrometer for the  $1.1-1.95 \mu\text{m}$  range. Along with FGS an IR Spectrometer (AIRS) is foreseen, providing low-resolution spectroscopy in two IR channels: Channel 0 (CH0) for the  $1.95-3.90 \mu\text{m}$  band and Channel 1 (CH1) for the  $3.90-7.80 \mu\text{m}$  range.

Finally, an Active Cooler System (ACS) including a Ne Joule-Thomson cooler is adopted to provide active cooling capability to the AIRS detectors working at cryogenic temperatures, below  $42\text{K}$ .

## 1.1 Orbit

The operational orbit of the Ariel spacecraft [2] is baselined as a large amplitude halo orbit around the Sun-Earth system 2<sup>nd</sup> Lagrangian (L2) point (refer to Fig. 1). This virtual point in space is located about  $1.5$  million km from the Earth in the anti-Sun direction, and is confirming the orbit of choice of many current, like JWST, and future (e.g. PLATO) astrophysical missions, because it offers the possibility of long uninterrupted observations in a fairly stable radiative and thermo-mechanical environment.

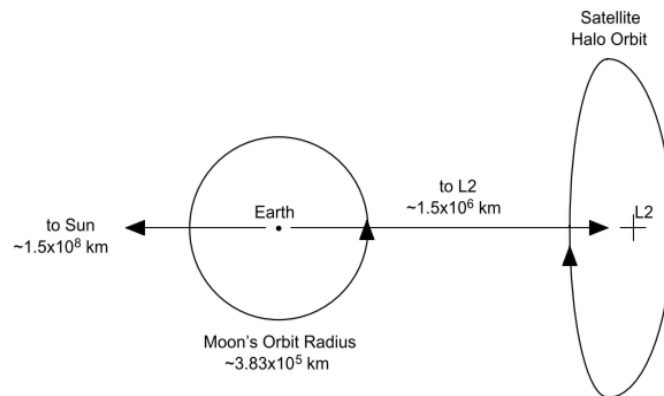


Figure 1. Ariel halo orbit around L2 with no eclipses allowed during the mission lifetime

The spacecraft will be launched by an Ariane A6.2 rocket from Kourou, in the French Guiana. A direct escape injection is planned in the baseline mission profile, being characterized by and involving different plasma environments. This trajectory foresees a single passage through the radiation belts, presently approximated by a somewhat worst case half orbit (10.5 hours) with perigee at  $300$  km (LEO environment) and apogee at  $64000$  km (GEO environment). An inclination of  $0$  degrees is assumed as a worst case.

The nominal mission duration is  $4$  years with a minimum extension of an additional  $2$  years, for a total mission duration of  $6$  years at least, for which the spacecraft shall be carefully designed. The space environment presents significant design challenges to all spacecraft, including the effects of interactions with the Sun radiation (sunlight) and charged particles owing to the surrounding plasma environment (refer to Fig. 2), potentially leading to dielectrics charging and unwanted ESD (Electro-Static Discharge) phenomena endangering the Payload operations and its data integrity.

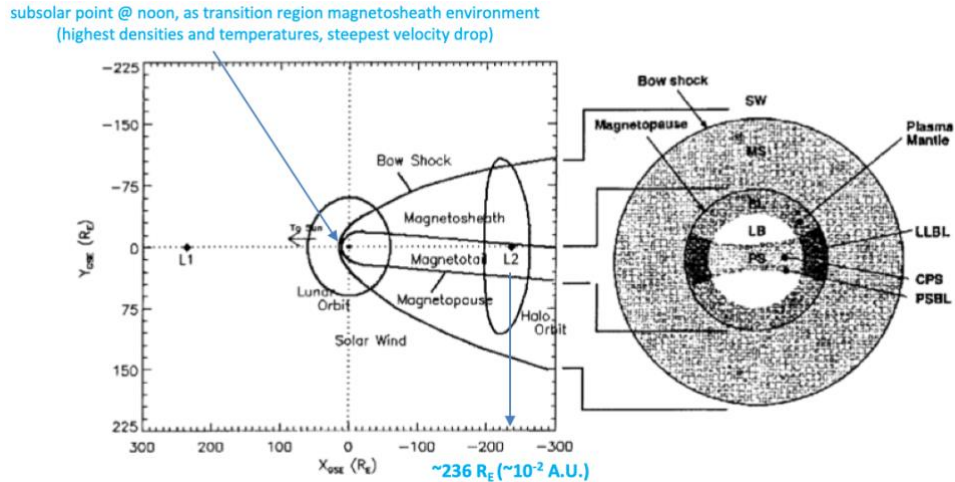


Figure 2. A sample halo orbit around L2 w.r.t. the dimensions of the Earth magnetotail and magnetosheath indicating the plasma regimes (SW: Solar Wind, MS: MagnetoSheath, BL: Boundary Layer, LB: Lobe, PS: Plasma Sheet, LLBL: Low Latitude Boundary Layer, CPS: Central Plasma Sheet, PSBL: Plasma Sheet Boundary Layer)

Here, we present some preliminary simulations and analyses about the Ariel Payload dielectrics surface charging along the transfer orbit from launch to L2, performed thanks to the exploitation of the EQUIPOT tool of the ESA's SPENVIS (SPace ENVIRONMENT Information System) suite, a w3-based ([www.spennis.oma.be](http://www.spennis.oma.be)) interface to model the space environment and its effects.

## 2. ARIEL PAYLOAD DESIGN, ENVIRONMENT AND MATERIALS

The Ariel Payload is conceived modular by design (refer to Fig. 3). The adopted baseline architecture splits the payload into two major sections, the cold payload module (PLM) and the items of the Payload hosted within the spacecraft service module (SVM), i.e. the warm units electronics.

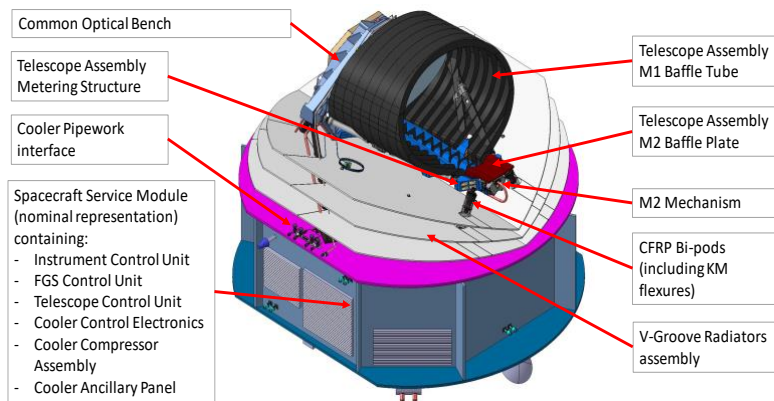


Figure 3. Illustration of the Ariel Payload Module (PLM, top) and Service Module (SVM, bottom) composing the whole Spacecraft

The PLM is supported by three bipods mounted onto the Payload Interface Panel (PIP). They are hollow cylinders, made of CFRP (*Carbon Fiber Reinforced Polymer*) filled with low thermally conductive rigid foam. Three Planck-like V-

Grooves (VGs) are adopted as high-efficiency passive radiant coolers, providing the first stage of the PLM cooling system. VGs are made by a simple honeycomb structure of Aluminum alloy, thermally connected to the three bipods (to intercept the conducted parasitic heat leaks through the mounting bipods) and are mechanically supported and thermally decoupled from the PIP by GFRP (Glass Fiber Reinforced Polymer) struts (refer to Fig. 4).



Figure 4. CFRP-made bipods and GFRP-made struts configuration as V-groove support (left); a bipod cross-section (right)

A preliminary surface charging analysis, by means of the EQUIPOT/SPENVIS tool [3], has been performed to demonstrate that, in case of the adoption of semi-conductive and dielectrics materials like CFRP and GFRP they don't pose threat to any equipment on the Payload and Spacecraft and the relevant risk associated with electrostatic discharges, due to charge build-up in the material, which may damage nearby equipment, is minimized. This risk depends on the surface area of the materials directly exposed to space and the unit/equipment configuration w.r.t. the orbit characteristics.

It is worth noting that general surface charging with following possible harmful electrostatic discharges is usually a problem in earth orbit at high altitude or polar latitude, especially when the spacecraft is subjected to periodic eclipses. The potential (voltage) ranges expected for Ariel are preliminary demonstrated as not critical and there should be no risk of any powerful discharge, due to the expected voltage differences between the plasma environment, the structure and selected materials, like semiconductors and dielectrics in particular. However, the computed ranges may raise concern for specific systems sensitive to potential fluctuations, accounting for different charging times.

The main plasma regimes experienced by the Ariel spacecraft are the solar wind and the outer magnetosphere, as described and quantified in Tables 1 to 3. The spacecraft is expected to spend a significant amount of time in both of these regimes [4].

In particular, the solar wind, the outer magnetosphere plasma environment and the plasma effects have to be properly assessed and characterized. These are indeed related to three distinct plasma regimes which can be identified around L2 [5], [6]. The Ariel spacecraft will spend most of its time in the solar wind and the magnetosheath and a small fraction of the time in the magnetotail. The ratio of time in these environments will depend on the actual orbit.

It should be noted that the boundaries between these regions at L2 show a large variability due to possible variations in the solar wind strength due to the solar cycle. The solar wind varies on time scales of tens of minutes to days – short, compared with the orbit of the Ariel spacecraft around L2 - meaning that within a single orbit the spacecraft is likely to encounter several different plasma regimes [7].

### 3. IN-SPACE DIELECTRICS AND SEMICONDUCTORS CHARGING MECHANISMS

A satellite hosting a net electric charge (positive or negative), due to the interaction with the surrounding plasma, as further described in the following sections, generates an electric field in accordance w.r.t the Gauss law as a result of the vector nature (central field) and analytical formulation of the field itself ( $\sim r^{-2}$ ). The satellite voltage level is associated to the electric field value, which strength is a function of the charge and fluctuations of the closer plasma environment [8].

Space plasma is generally assumed as neutral (as a reasonable assumption on large spatial and temporal scales) and, from literature, the ambient plasma potential (or reference voltage level) is defined as zero (refer to Fig. 5):

$$\Phi_p = 0$$

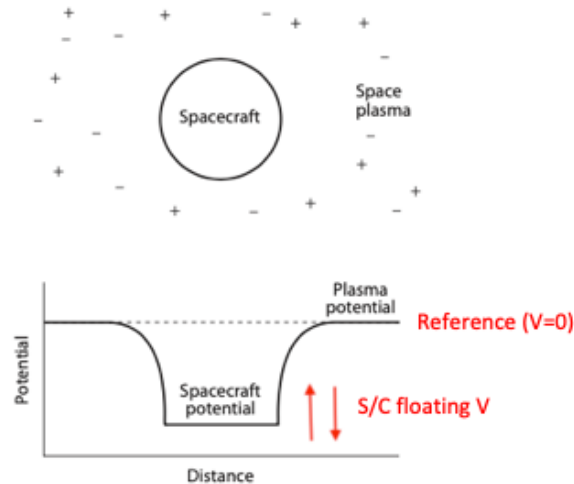


Figure 5. Spacecraft floating voltage level vs plasma reference voltage

A basic terminology related to spacecraft charging, adopted by this work, is introduced by [8]:

- For a conducting spacecraft, the charges are on the surfaces. This charging situation is called *surface charging*.
- A uniformly charged spacecraft has only one potential,  $V_s$ . This situation is called *uniform charging* or *absolute charging*.
- For a spacecraft composed of electrically separated surfaces, the potentials may be different on different surfaces. The potentials depend on the surface properties and on the environment, which may be non-isotropic. In this case, we have *differential charging*.
- If a spacecraft is covered with connected conducting surfaces (i.e., spacecraft ground or frame) and some unconnected or nonconducting surfaces, the charging of the frame is called *frame charging*.
- When the ambient electrons ( $e^-$ ), protons ( $p^+$ ) and heavier ions ( $i^{++}$ ) are very energetic (MeV or higher), they can penetrate deep into dielectrics. This situation is called *deep dielectric charging*, or *bulk charging*.

For a conductive, non-dielectric material, an hitting charged particle penetrating into it moves quickly to the surface due to the Coulomb repulsion and to the internal material mobility of the charges. Therefore, for conductors, surface charging can occur, but deep conductor charging does not occur. In dielectrics, on the other hand, both surface charge and deep charge phenomena can occur. Semiconductors, in turn, may have longer charges re-organization (when compared to conductors) due to their different mobility within the material.

### 3.1 Surface charging process

Surface charging processes occur due to the interaction of the spacecraft exposed surfaces to the plasma environment, solar radiation, high-energy electrons and electromagnetic fields in general. In particular, the main cause of the surface charging processes is due to the differential flows of electrons and ions characterizing the surrounding environment.

As electrons have higher speeds due to their lower mass w.r.t. other ion species, but the same plasma thermal energy ( $kT_i = kT_e$ ), when a reference (unitary) surface is not directly exposed to sunlight it charges negatively, since it intercepts on average more electrons than ions during a selected timeframe. When the satellite is, in turn, exposed to direct sunlight,

the electrons photoemission can become so significant as to positively charge the reference area. Both these processes shall be carefully considered when the satellite orbit is subjected to eclipses.

At equilibrium, the selected surface behaves like a circuitual node so that it is possible to apply the Kirchoff's second law, which states that for each node at equilibrium, the sum of the incoming currents shall match the sum of the outgoing currents. This implies that the surface voltage level shall be such that the sum of all currents vanishes. A vehicle that moves through the space plasma reaches its electrical equilibrium by charging its surfaces in such a way as to null the total current of a reference circuitual node. The equilibrium conditions define in that way the voltage level of the reference surface (e.g. a representative patch) builds-up with respect to the surrounding plasma.

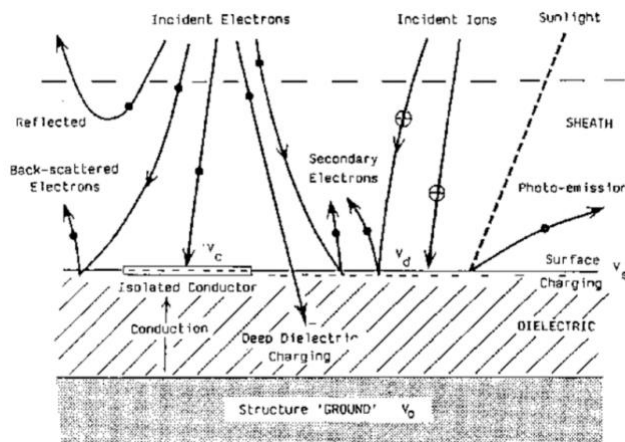
A generic spacecraft can be composed of conductive, insulating, partially insulating and/or semiconducting materials. Due to the mobility of the charges in the conductive materials, a global balance is established, while for the insulating materials the balance is in turn locally established.

During the transients, however, the Kirchoff's law cannot be applied and it is necessary to take into account the characteristic charging times (of the order of a few milliseconds) linked to the capacitance values (a spherical object with a diameter of 1m has a capacitance C of the order of  $10^{-10}$  Farad) and to the fluxes of the involved charged particles (for comparison the characteristic fluctuation times of the local plasma are much shorter, since they are related to the inverse of the plasma frequencies).

In the process leading to equilibrium, the electrons and ions (mainly protons, but also heavy ions) flows from the neutral (on large scales) plasma environment shall be considered (refer to Fig. 6), as well as the secondary photoemission phenomena due to the photoelectric effect, when the spacecraft is subjected to direct sunlight. That is why single or recurring eclipses have to be considered, as well as back-scattered electrons, by means of the following equation:

$$I_{NET}(V) = I_E(V) - [I_I(V) + I_{SE}(V) + I_{SI}(V) + I_{BSE}(V) + I_{PH}(V)] + I_C(V)$$

whose terms are fully defined in Fig. 6 legend.



Legend:

- V: surface/patch voltage level w.r.t. plasma environment
- $I_{NET}$ : net sum of incoming and outgoing currents
- $I_E$ : incoming environmental electrons current
- $I_I$ : incoming environmental ions current
- $I_{SE}$ : secondary electrons outgoing current (due to  $I_E$ )
- $I_{SI}$ : secondary electrons outgoing current (due to  $I_I$ )
- $I_{BSE}$ : back-scattered electrons outgoing current (due to  $I_E$ )
- $I_{PH}$ : photoelectrons emission current (due to impinging sunlight)
- $I_C$ : conduction current from the reference structure (ground reference for the spacecraft)

Note: incoming/outcoming electrons/ions are indicated in the picture on the right by different symbols

Figure 6. Surface charging mechanisms and involved currents

Usually,  $I_C$  can be neglected w.r.t. the involved currents; however, for the sake of completeness, it has been considered for the Ariel Payload simulations carried out with the ESA SPENVIS simulator.  $I_I$ ,  $I_{SE}$ ,  $I_{SI}$ ,  $I_{BSE}$  and  $I_{PH}$  are considered as positive currents, since they are related to electrons leaving the surface and incident positive ions. On the contrary,  $I_E$  acts as a negative current as it is linked to incident electrons on the surface or reference patch.

The equilibrium condition is therefore given by:

$$I_{NET} = 0$$

### 3.2 Bulk charging process

If the incident electrons on the spacecraft are characterized by high energies (of the order of some MeV or higher), they can penetrate deeply inside the materials and settling there. These electrons can enter the dielectrics and remain there as stationary charged particles for a long time. After a prolonged period of material hitting, the electrons collected into the dielectric can produce a not negligible electric field, if the rate at which they are deposited exceeds the rate at which they are redistributed. If the field is high enough to overcome the dielectric strength of the material, it can give rise to a localized internal discharge due to overloading conditions inside the dielectric. When a local overload occurs, ionization channels within the dielectric can rapidly develop leading to current flows, which in turn generate further ionization and heat dissipation. The avalanche ionization process just described causes an electrical discharge throughout the material. This phenomenon is called punch-through discharge. As a result, sensitive electronic equipment can be seriously damaged [9].

Although the densities of high-energy electrons in interplanetary space far from the Sun are usually low and the above described events are pretty rare, should they occur, they could even lead to the loss of the vehicle and the entire mission.

## 4. THE SPENVIS/EQUIPOT TOOL

SPENVIS is an online simulator and analysis tool aimed at defining coherent and structured models of the space environment concerning multiple types of analyses, including surface and bulk charging, requiring for some tools like EQUIPOT no input orbit files (simply described by the plasma environment input parameters) and neglecting geometrical effects (no input CAD models and/or .stp files).

A finite elements model (FEM) three-dimensional simulation of surface charging processes is, in principle, an extremely complicated procedure and an example of a dedicated tool performing such a kind of task is NASCAP (NASA Charging Analyzer Program). NASCAP is a very sophisticated software, whose adoption is outside the scope of this work, and for this reason a simpler 1D simulator<sup>†</sup> developed by ESA, EQUIPOT, owing to the SPENVIS suite, was used.

EQUIPOT has been basically designed for a quick assessment of the likelihood of surface charge formation. It does not rely on the reproduction of a fully realistic geometry of the problem but assumes a simplified model, based on a small isolated area (i.e. a patch) with a local planar geometry on the surface of a spherical vehicle with a diameter of 1m and it computes the current components through the patch area at equilibrium ( $I_{NET} = 0$ ) in order to define the potentials of the patch itself and of the structure with respect to the surrounding plasma, as V reference. The software also calculates the charging times, producing plots of voltage levels versus time.

The materials composing the vehicle and the patch are defined and set in EQUIPOT by the user, as well as the plasma environment in which the mission will operate through the definition of the energy spectra for the electron and ion flows and their Maxwellian velocity distributions (or energies). For a correct and representative definition of the plasma environment, up-to three thermal spectra for the electrons, defined by a density and a temperature and up-to three thermal spectra for the ions, defined by a density, a temperature and an average particles mass can be set in the simulator. In addition, or alternatively, a flux spectrum for electrons, defined as a series of energies and fluxes, and/or a flux spectrum for ions, defined as a series of energies and fluxes plus a mass can be set.

---

<sup>†</sup>For passive Spacecraft, i.e. with no ions engines nor intrinsic ions/electrons sources



The net current density ( $I_{NET} \rightarrow J_{NET}$ ) on a surface involves several components used by EQUIPOT to perform a numerical integration process (refer to previous equation). The secondary currents are determined using the appropriate yields, which accuracy (for secondary electrons) is fundamental for the analysis of the surface charging computation, and EQUIPOT offers four different formulations of the emission yields (Burke, Whipple, Katz and Sims models). Although the algorithm used for the Whipple formulation is more stable, no significant differences were found for the alternative choices.

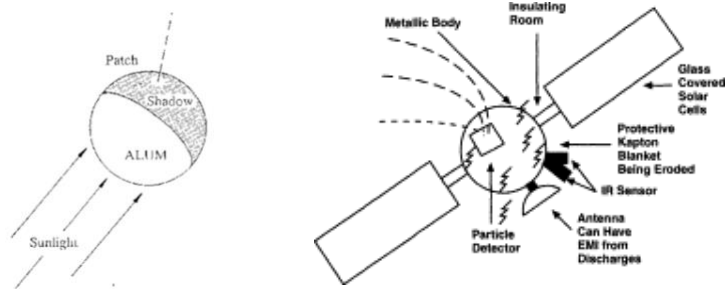


Figure 7. A spacecraft model with a reference patch geometry and orientation w.r.t. the impinging sunlight (left); comparison w.r.t. a more realistic satellite hosting many subsystems and different kind of materials (right)

Once the environment and materials have been defined, the EQUIPOT software runs determining currents and voltages levels by obtaining the equilibrium potentials of both the structure and patch. The adopted code uses a step-by-step algorithm for calculating the potential that dynamically controls its incremental values in order to minimize the net current and quickly converge towards the equilibrium, assuming a single solution for the boundary assumption ( $I_{NET} = 0$ ).

### 5. INPUT DATA FOR SURFACE CHARGING ANALYSES

In the following tables (they refer to ECSS-E-ST-10-04C, 15 Nov 2008 issue) are reported the inputs data representing the charged particles energies that have been taken into account to describe the Solar Wind, the Earth magnetosheath, lobe (magnetotail) and plasma sheets, as defined in the Ariel Environmental Specifications from ESA and ECSS (European Cooperation for Space Standardization) applicable standards as well.

Parameter	At the Earth (1AU)	Range 5%-95% Limit	
Density ( $cm^{-3}$ )	8.7	3.0	20
Speed ( $km\ s^{-1}$ )	468	320	710
$T_p$ (K)	$1.2 \times 10^5$	$0.098 \times 10^5$	$3.0 \times 10^5$
$T_e$ (K)	$1.0 \times 10^5$	$0.89 \times 10^5$	$2.0 \times 10^5$
$T_{alpha}$ (K)	$5.8 \times 10^5$	$0.60 \times 10^5$	$15.4 \times 10^5$
$\lambda$ (m)	7.3	-	-
$N_{alpha}/N_{proton}$	0.047	0.017	0.078

Table 1. Solar Wind parameters

Table H-6: Typical magnetosheath plasma parameters

Local time	Speed ( $km\ s^{-1}$ )	$T_p$ (K)	$T_e$ (K)	Density ( $cm^{-3}$ )
12 noon	50	$2 \times 10^6$	$2 \times 10^6$	35
06 hours	350	$1 \times 10^6$	$1 \times 10^6$	20

NOTE From [RD.116]

Table 2. Magnetosheath plasma parameters in near-Earth environment for subsolar point (refer to Fig. 2) at noon and from midnight to six a.m.

**Table H-7: Typical plasma parameters around L2**

	<b>n cm<sup>-3</sup></b>	<b>Ti eV</b>	<b>Te eV</b>	<b>V km s<sup>-1</sup></b>
Magnetosheath	1,0	80	26	312
Lobe	0,1	540	180	60
Plasma sheet	0,15	610	145	72

NOTE: Taken from 50% cumulative probability measurement from Geotail [RD.6])

Table 3. Plasma parameters around L2

For surface charging analyses only charged particles up to 500 KeV have been considered in this study context, as main responsible for surface charging effects. Bulk dielectrics charging, presently not considered, is normally caused by particles with higher energies.

### 5.1 Input parameters selection

In order to perform realistic surface charging simulations related to the CFRP-based [10] bipods by means of EQUIPOT, the satellite main structure and the V-shaped metallic (Al-made) radiators, along with a CFRP patch, were initially selected as input data for the involved materials. The patch orientation was also chosen accounting for the bipods geometry (45 degrees) w.r.t. the PIP panel, S/C Service Module and impinging sunlight.

Simulations were, then, performed for the GFRP-made struts and the structure by selecting a generic insulator as a reference material, defined by the user as the worst case about the surface resistivity of the GFRP composite material.

For the space plasma environment, a high altitude orbit (GEO) [11] has been selected and exposed to direct sunlight, as a consequence of the fact that both the insertion trajectory and the orbit around L2 will be excluded from the eclipse zones due to the presence of the Earth or the Moon. Only for the first hours of flight (12/noon, see Table 2) a low altitude orbit (LEO) was selected.

Concerning the plasma environment during the transient ascent, some simulations were performed in relation to the expected injection trajectory towards L2, with a passage through the magnetosphere and Van Allen belts.

For the injection trajectory, the available input data in the ECSS reference documentation were chosen for the thermal spectrum (refer to Tab. 2), while concerning the fluxes relating to protons and electrons, the data from satellites AE-8 and AP-8 (<https://ccmc.gsfc.nasa.gov/modelweb/models/trap.php>) [12] were taken, for energies below 500 keV.

For the final orbit in L2 (halo orbit) the Solar Wind data obtained from the Ariel Environment Specification (source ESA, refer to Tab. 1) and the relevant data for the magnetopause and the magnetotail from ECSS (Tab. 3) were used as thermal spectra. Simulations in plasma environments representing both the magnetopause and magnetotail were then performed in order to compute the expected patch and structure voltage levels.

## 6. SIMULATIONS AND ANALYSES

With reference to the first flight hours of the mission (i.e. launch window around 12:00 local time, as main assumption, to be confirmed), the following results (voltage levels w.r.t. plasma vs time) for the S/C structure and the P/L bipods were obtained:

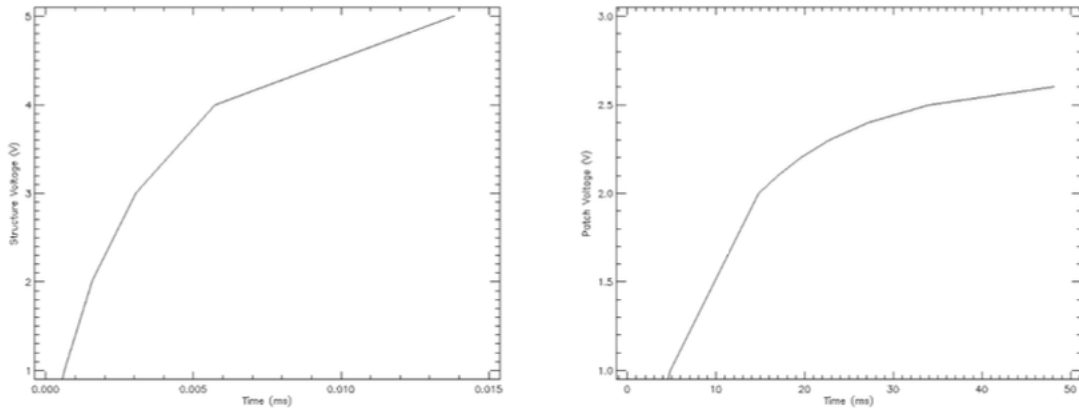


Figure 8. Structure and bipod-representative patch voltage levels vs charging time (first hours of flight)

and, for the structure and V-grooves struts:

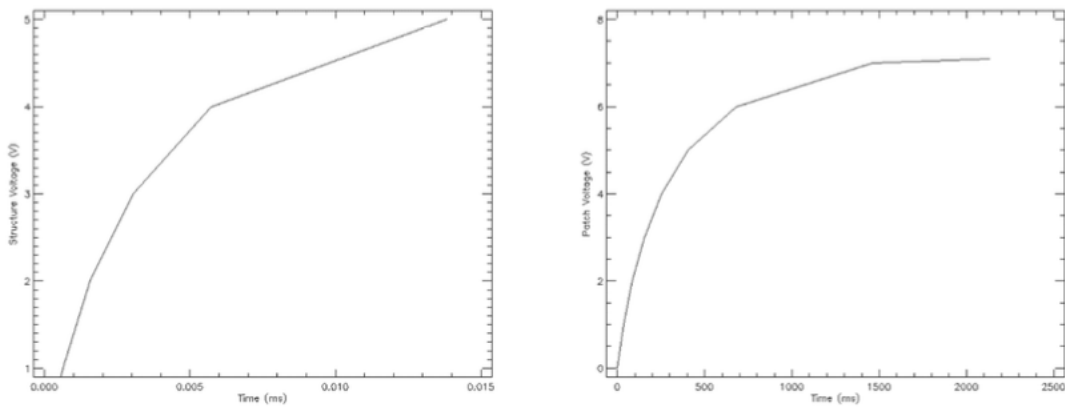


Figure 9. Structure and VG strut-representative patch voltage levels vs charging time (first hours of flight)

Concerning the L2 environment, simulations were initially performed only accounting for the data relating to the magnetopause, obtaining the following results for the S/C structure and P/L bipods:

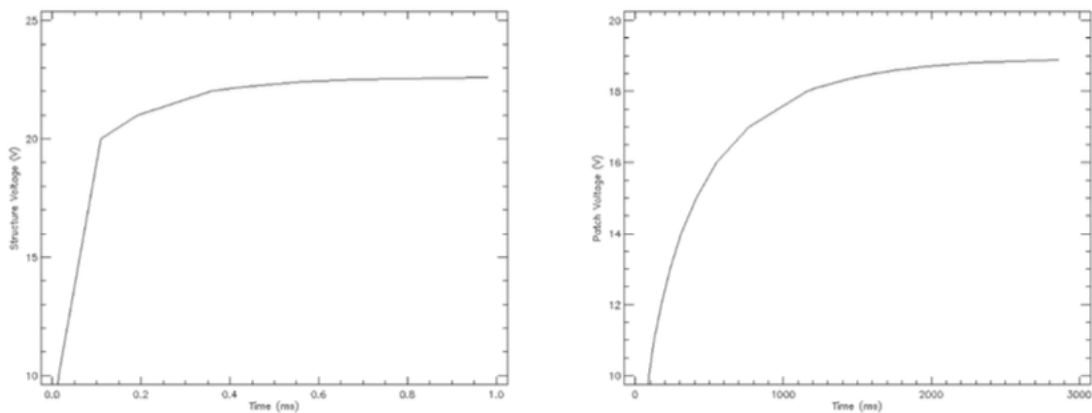


Figure 10. Structure and bipod-representative patch voltage levels vs charging time (L2 magnetopause)

and, for the structure and V-grooves struts:

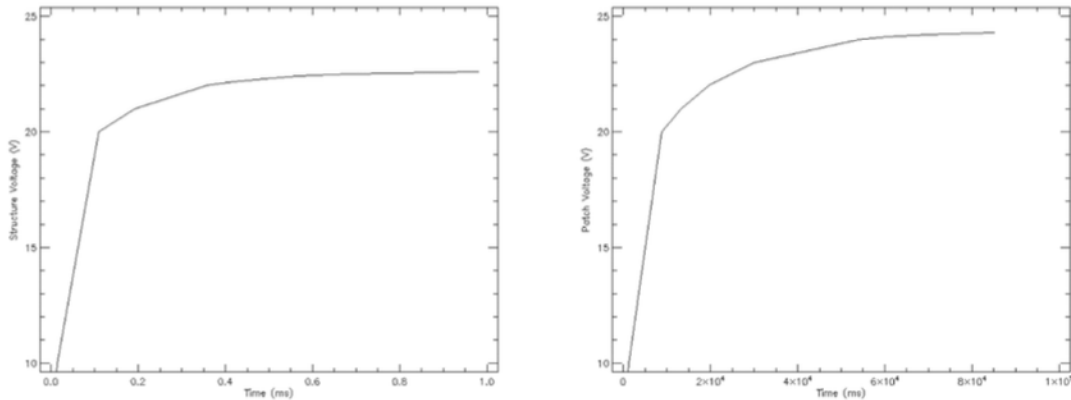


Figure 11. Structure and VG strut-representative patch voltage levels vs charging time (L2 magnetopause)

More realistic simulations were, then, performed considering the effects of the Solar Wind, in addition to the magnetopause, obtaining for the S/C structure and P/L bipods:

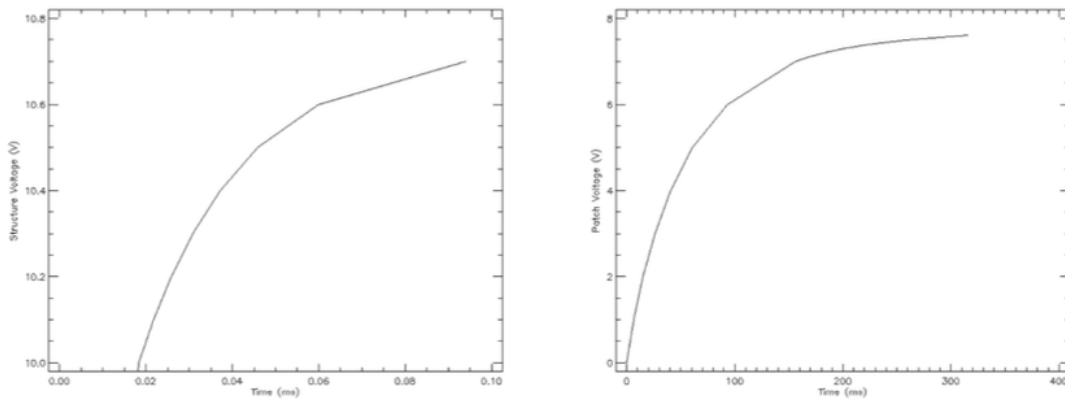


Figure 12. Structure and bipod-representative patch voltage levels vs charging time (L2 magnetopause plus Solar Wind)

and, for the structure and V-grooves struts:

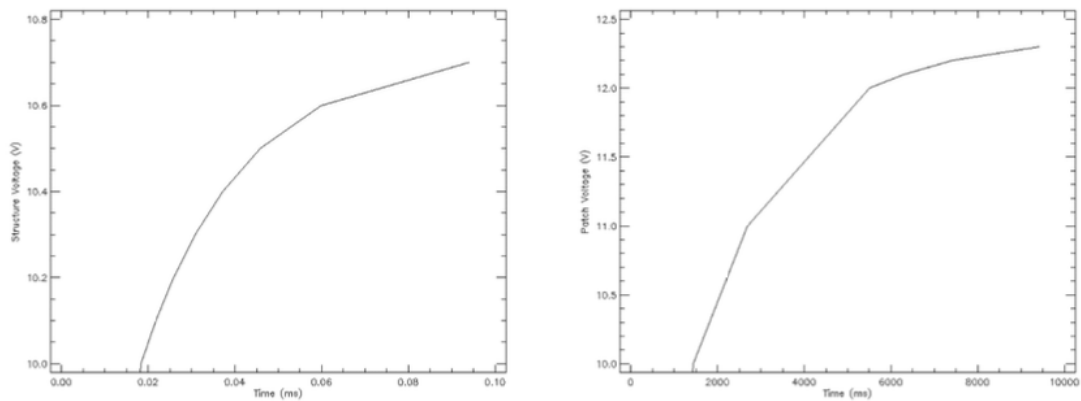


Figure 13. Structure and VG strut-representative patch voltage levels vs charging time (L2 magnetopause plus Solar Wind)

Finally, simulations were performed considering the effects of the Solar Wind and the terrestrial magnetotail plasma environment on the S/C structure and bipods:

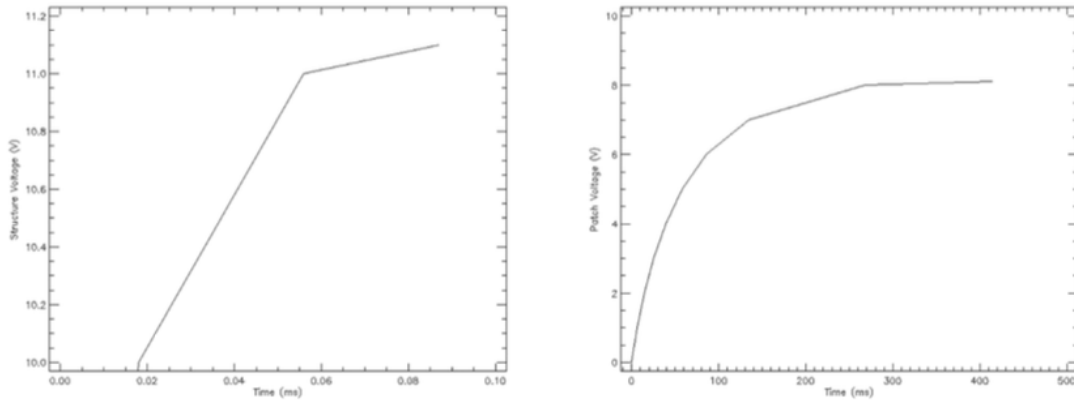


Figure 14. Structure and bipod-representative patch voltage levels vs charging time (Solar Wind and Earth magnetotail)

and, for the structure and V-grooves struts:

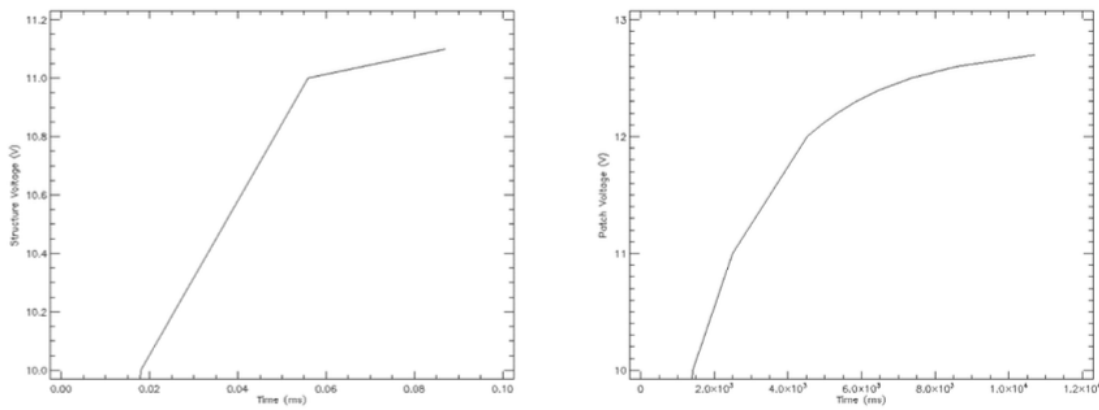


Figure 15. Structure and VG strut-representative patch voltage levels vs charging time (Solar Wind and Earth magnetotail)

According to the EQUIPOT reference manual and to the ECSS standard [13], [14] on the interpretation of the achieved results (potentials and charging times<sup>‡</sup>), when the voltage difference between the patch and the metallic (Al) S/C structure is below 100V, as we found, there is no real risk of electrostatic discharges between them and to the surrounding plasma, assumed as the V=0 reference.

Even if the charging times, linked to the different electrical properties of the involved materials and related to the selected surfaces differs by one or more orders of magnitude, there should not be a real risk of ESDs [15], since at each time the voltage differences are limited to a range of a few V to a few tens of V (also accounting for the uncertainties), but ultimately below the 100V threshold.

## 7. CONCLUSIONS

The performed analyses and simulations, accounting for the SVM bottom panel hosting the spacecraft solar arrays, always illuminated by the sun light (i.e. no eclipses allowed), confirm that the expected voltage ranges for the exposed

<sup>‡</sup>The charging process time and V vs t curve shape is basically due to an RC circuit schematization and its RC time constant

S/C structure, dielectrics (e.g. GFRP) and semiconductors-like materials (e.g. CFRP, in terms of its surface resistivity value) are not critical (all values below 100V, as differential voltage levels and w.r.t. the plasma reference potential) and there is no considerable risk of dangerous electrostatic discharges. However, as preliminary results, the computed values may still raise some concerns for specific systems sensitive to voltage fluctuations, that shall be further assessed at Payload and Instrument level (e.g. exposed cryoharness to space) accounting, in particular, for the different involved materials, their properties and charging times.

As a rule of thumb, for the exposed cryoharness external jackets (when adopted over the external conductive shields for their insulation, preserving electrical performance like grounding rules), we advise for the adoption of ETFE-like (ethylene tetrafluoroethylene) materials or the use of anti-ESD epoxy primers (e.g. conductive carbon black) or anti-ESD coatings, accounting for their thermal properties (emissivity) and the Payload heat leaks and thermal dissipation needs.

Additional effects due to possible deep dielectrics charging caused by energetic particles impinging on the Spacecraft should be also assessed in the near future by the spacecraft provider (Airbus DS), as not covered by the present Payload surface charging analyses.

## 8. ACKNOWLEDGEMENT

This study has been supported by the *Italian Space Agency (ASI)* thanks to the ASI-INAF agreement n. 2021-5-HH.0 “*Scientific activity for the Ariel Mission – B2/C Phases*”

## REFERENCES

- [1] Ariel Mission Consortium (AMC), Ariel Definition Study Report (Red Book), 2020
- [2] L. Puig, The phase A study of the ESA M4 mission candidate Ariel, 2018
- [3] SPENVIS/EQUIPOT User Manual, <https://www.spennis.oma.be/>
- [4] D. Rodgers et al., Ariel Environment Specification, ESA-ARIEL-EST-SP-001, 2018
- [5] J. I. Minow et al., Charged particle environment for NGST: L2 plasma environment statistics, 2000
- [6] S. W. Evans, Natural environment near the Sun/Earth-Moon L2 libration point, 2003
- [7] T. Ondoh, K. Marubashi, Science of space environment, 2001
- [8] Shu T. Lai, Fundamentals of Spacecraft Charging: Spacecraft Interactions with Space Plasmas, Princeton University Press, 2011
- [9] T. Mikaelian, Spacecraft Charging and Hazards to Electronics in Space, 2001
- [10] Q. Zhao, Review on the Electrical Resistance/Conductivity of Carbon Fiber Reinforced Polymer, 2019
- [11] J.L. Roeder, Specification of the Plasma Environment at Geosynchronous Orbit in the Energy Range 87 eV to 288 keV, 1994
- [12] J. I. Vette, The AE-8 Trapped Electron Model Environment, 1991
- [13] ECSS-E-ST-10-04-C, Space environment, 2008
- [14] ECSS-E-ST-20-06C Rev.1, Spacecraft Charging, 2019
- [15] J. A. Roth, Electrostatic Discharge in Spacecraft Materials, 2009